# Coalescence delay of microbubbles on superhydrophobic/superhydrophilic surfaces underwater

Mizuki Tenjimbayashi, Yudai Kawase, Kotaro Doi, Chen Xian Ng, and Masanobu Naito

View Online        Export Citation        CrossMark

## ARTICLES YOU MAY BE INTERESTED IN

# Coalescence delay of microbubbles on superhydrophobic/superhydrophilic surfaces underwater

Mizuki Tenjimbayashi,[1,a)] Yudai Kawase,[1] Kotaro Doi,[2] Chen Xian Ng,[1] and Masanobu Naito[1,a)]

[1]*Research and Services Division of Materials Data and Integrated System (MaDIS), National Institute for Materials Science (NIMS), 1-2-1 Sengen, Tsukuba Ibaraki 305-0047, Japan*
[2]*International Center for Young Scientists (ICYS), National Institute for Materials Science (NIMS), 1-2-1 Sengen, Tsukuba Ibaraki 305-0047, Japan*

Inspired by penguins, the formation of an air film on surfaces underwater has been well-researched for the potential reduction of drag. However, the features that contribute to drag reduction of penguins are not only the formation of an air layer but also the flow of bubbles along the air layer; basic investigation of the wetting dynamics of a bubble scattered in an underwater environment has been overlooked. The focus of our research was microbubble contact on superhydrophobic/superhydrophilic surfaces underwater. Unlike the adhesion of mist in air, a "coalescence delay" is observed when bubbles make contact, which influences the deposition dynamics of an air film. The "coalescence delay" is proportional to the size of the bubbles. This study is helpful to understand air/solid/water systems as well as the drag reduction. *Published by AIP Publishing.* https://doi.org/10.1063/1.5038910

Nature has always inspired ideas for the design of superwetting materials (*e.g.,* lotus, nepenthes and water strider).[1–3] Some experimental and theoretical investigations have shown that the penguin-inspired approach of introducing an air film on a superhydrophobic surface is an effective method for the drag reduction underwater.[4–8] However, the features of a penguin's skin are not only the formation of an air layer but also the flow of bubbles along the air layer. Therefore, a real analogue can be considered to be the interfacial dynamics of superhydrophobic surfaces in bubbles scattered underwater.[9] Despite the development of superwetting materials against air in underwater conditions as well as their potential application in sensors, transportation, and reactors,[10,11] the wetting dynamics of bubbles scattered underwater have not been investigated.

Herein, we prepared superhydrophobic and superhydrophilic surfaces and studied the wetting dynamics of contacting microbubbles scattered underwater, as shown in Fig. 1(a). The bubbles were formed through the electrolysis of water. A carbon steel plate and a carbon plate were used as a working electrode and a counter electrode, respectively. To increase the electrical conductivity, $2.0 \times 10^{-3}$ M $K_2SO_4$ was added to the water. The bath water-vapor interfacial tension was $71.9 \pm 3.6$ mN m$^{-1}$ ($n = 15$), and the pH value was 7.8. An applied current of 0.2–0.3 mA generated submicrometer-sized bubbles (diameter: $54.1 \pm 29.6 \mu m$, $n = 1000$, see supplementary material). The formed bubbles moved in a vertical direction to the substrates by buoyancy at a speed of $\sim 10$ mm s$^{-1}$ [Fig. 1(b)]. Figure 1(c) shows that the impact speeds of the microbubble to the substrates were mostly uniform (within 5 mm s$^{-1}$). A few bubbles moved at a higher speed owing to the coalescence on the working electrode, although this was extremely rare.

A superhydrophobic surface was prepared by dipping a glass plate into a mixture of zinc oxide micro-tetrapod powder and polydimethylsiloxane (PDMS). The zinc oxide powder was used for roughening the surface structure, and PDMS was used because of its low surface energy. A superhydrophilic surface was prepared by treating a glass plate with plasma. Figure 2 shows the wettability of the different surfaces that were prepared. Theoretically, the sum of the Young contact angle of water and air is approximately 180°.[12] Therefore, as the more hydrophobic the solid gets,
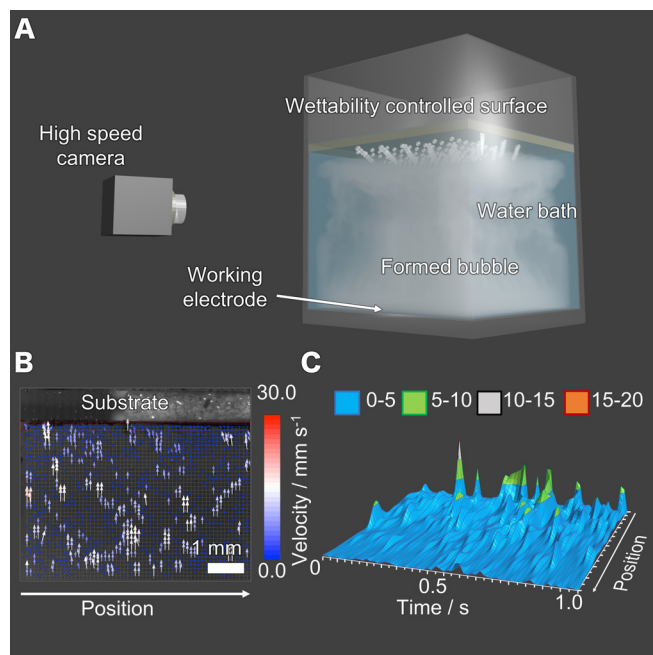


FIG. 1. (a) A schematic diagram of the experiment. The wettability-controlled surface is faced down in a water bath. Bubbles are formed by the electrolysis of water. The bubble-coating interface is observed using a high-speed camera. (b) Gas bubble velocity distribution mapping. (c) Time-lapse distribution of the impact velocity of the bubbles.

a)Authors to whom correspondence should be addressed: TENJIMBAYASHI. Mizuki@nims.go.jp and NAITO.Masanobu@nims.go.jp

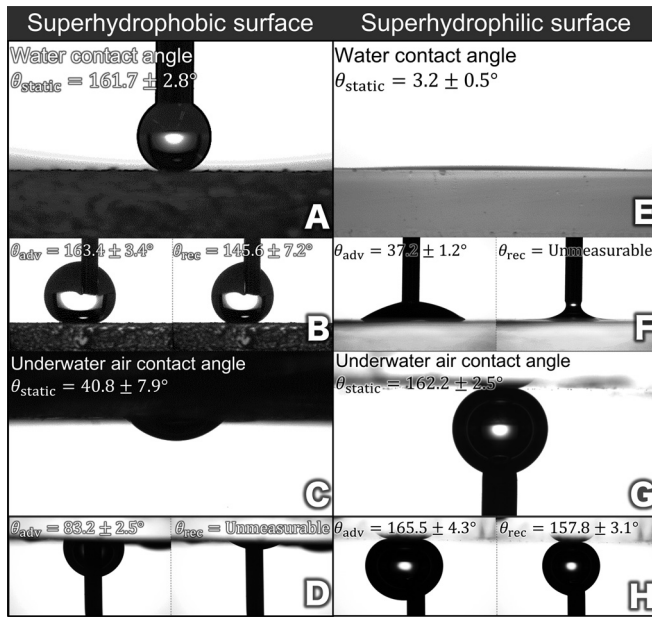| Superhydrophobic surface | | Superhydrophilic surface | |
|---|---|---|---|
| Water contact angle $\theta_{\text{static}} = 161.7 \pm 2.8°$ | | Water contact angle $\theta_{\text{static}} = 3.2 \pm 0.5°$ | |
| **A** | | **E** | |
| $\theta_{\text{adv}} = 163.4 \pm 3.4°$ | $\theta_{\text{rec}} = 145.6 \pm 7.2°$ | $\theta_{\text{adv}} = 37.2 \pm 1.2°$ | $\theta_{\text{rec}} =$ Unmeasurable |
| **B** | | **F** | |
| Underwater air contact angle $\theta_{\text{static}} = 40.8 \pm 7.9°$ | | Underwater air contact angle $\theta_{\text{static}} = 162.2 \pm 2.5°$ | |
| **C** | | **G** | |
| $\theta_{\text{adv}} = 83.2 \pm 2.5°$ | $\theta_{\text{rec}} =$ Unmeasurable | $\theta_{\text{adv}} = 165.5 \pm 4.3°$ | $\theta_{\text{rec}} = 157.8 \pm 3.1°$ |
| **D** | | **H** | |

FIG. 2. Wettability of a superhydrophobic surface (a)–(d) and superhydrophilic surface (e)–(h). The wettability analyses were the static water contact angle in air [static: (a) and e and dynamic: (b) and (f)] and underwater air contact angle [static: (c) and (g) and dynamic: (d) and (h)]. ($n = 10$).

the more aerophilic the solid becomes.[10,11,13–15] In the case of our samples, the superhydrophobic surface was aerophilic underwater and capable of forming an air film (*i.e.,* unmeasurable receding contact angle in a decreasing bubble volume) as shown in Figs. 2(a)–2(d), whereas the superhydrophilic surface was superaerophobic underwater and the adhesion of the bubble was relatively low, as shown in Figs. 2(e)–2(h) (*i.e.,* $W_{\text{ad}} = \gamma_{\text{LV}}(1 + \cos\theta)$, where $W_{\text{ad}}$ denotes the adhesion work, $\gamma_{\text{LV}}$ the liquid vapor interfacial tension, and $\theta$ the droplet contact angle).[16] Thus, we anticipated that the wetting dynamics of the scattered bubbles underwater could correspond to mist adhesion in air, in which microbubbles simply coalesce on contact with other bubbles or the air film and grow.[17]

Interestingly, unlike the mist adhesion in solids or liquids in air, we noticed that there was a delay between the contact and coalescence of bubbles (termed "coalescence delay"), which influenced the deposition mechanism of the bubbles on the surface. As shown in Fig. 3(a), microbubbles uniformly adhered onto the superhydrophilic surface (see supplementary material). This phenomenon was owing to a "coalescence delay". When a floating bubble (bubble I) driven by a buoyancy force ($F_{\text{b}}$) comes into contact with a bubble that is adhered on the surface (bubble II), bubbles I and II do not coalesce owing to the coalescence delay and bubble I rolls along the curvature of bubble II, as schematically shown in Fig. 3(b) (left). We defined the time taken by bubble I to adhere onto the surface as $t_{\text{ad}}$. On the superhydrophilic surface, the highest $t_{\text{ad}}$ was 20 ms, which was much smaller than the coalescence delay time ($t_{\text{d}}$) of most of the bubbles observed. In the case $t_{\text{ad}} < t_{\text{d}}$, the bubbles adhered on the surface rather than coalesce with other bubbles. In contrast, on a superhydrophobic surface, an air film was formed, first owing to its wettability, and bubbles that float along the air film were absorbed by the air film. When

bubble III comes into contact with the air film, a coalescence delay occurs, and bubble III starts to roll along the air film. However, the bubble adhesion time is larger than the coalescence delay time ($t_{\text{ad}} > t_{\text{d}}$) owing to the large surface area of the air film. Thus, bubble III is absorbed by the air film before adhering onto the solid surface.

When a coalescence delay occurs, the bubble "hovers" on the air film surface (*i.e.,* contact angle ≈180°). This phenomenon indicated that a thin water layer existed between the bubble and the air film. Therefore, the delay is the lifetime of the thin water film. Recently, some reports performed air film mediated hovering of the liquid droplet.[18,19] Comparing the bubble coalescence underwater with the corresponding liquid droplet coalescence in air, the difference between the thin film conditions was the mass of the bubble/droplet and the viscosity of the surrounding space. For bubbles to coalesce underwater, the bubble must first penetrate the thin water film; however, the coalescence time is delayed because of the small momentum of the bubbles and the higher viscosity of the water compared with that of air. This phenomenon indicated that the delay time was in a positive correlation with the buffering time of the energy dissipation by interfacial change through coalescence.[20] The dissipation energy through coalescence ($E_{\text{dis}}$) is expressed as $E_{\text{dis}} = \Delta E_{\text{kin}} + \Delta E_{\text{interf}} + E_{\text{vis}}$,[21] in which $\Delta E_{\text{kin}}$ is the change in the kinetic energy ($\sim \rho u^2 r^3$, in which $\rho$ is the bubble density, $u$ is the bubble velocity, and $r$ is the radius of the bubble), $\Delta E_{\text{interf}}$ is the change in the interfacial energy ($\sim -\pi\gamma_{LV}r^2$ as long as the size of the air film is much larger than the size of the bubble), and $E_{\text{vis}}$ is the viscous dissipation energy ($\sim \Psi\rho^{-0.5}\Delta\mu\gamma_{LV}^{0.5}r^{1.5}$, in which $\Psi$ is the scale factor of the thin water film, $\rho$ is the gas density, and $\Delta\mu$ is the difference in viscosity between the gas and water). The bubbles used in this study were obviously smaller than the capillary length ($r < l_{\text{c}}^{\text{w}} = \gamma_{LV}^{0.5}\rho_{\text{w}}^{-0.5}g^{-0.5} \approx 2.7\,\text{mm} \ll l_{\text{c}}^{\text{g}} = \gamma_{LV}^{0.5}\rho_{g}^{-0.5}g^{-0.5} \approx 286.2\,\text{mm}$, in which $l_{\text{c}}$ is the capillary length and $g$ is the gravitational acceleration); therefore, the gravitational influence and the change in the momentum energy could be ignored. In addition, the mass of the bubble is small; therefore, the kinetic energy can be neglected in this experiment ($\Delta E_{\text{kin}} \approx 0$). Considering the coefficients in the approximation formula of the plot in Fig. 3(c), the measurement was reasonable in terms of the coefficient of $r^3$ being almost 0, which means that there is no influence of kinetic energy on the delay time. Thanks to the large value of $\Delta E_{\text{interf}}$ and $E_{\text{vis}}$, a coalescence delay was apparently observed under the studied conditions, and a positive correlation between the bubble size and the delay time was obtained. We confirmed that a relatively large bubble ($2r \approx 2.1\,\text{mm}$) was not absorbed in the air layer $t_{\text{d}} > t_{\text{ad}}$ even on a superhydrophobic surface, as shown in Fig. 3(d). The lifetime of the target bubble highlighted in yellow in Fig. 3(d) was ≈1700 ms, whereas the adhesion time on the air layer was ≈140 ms, which fulfills the criterion of $t_{\text{ad}} > t_{\text{d}}$. The bubble rolls on the air film and settles next to the neighboring air film. After 1732 ms, the air film and the bubble coalesced.

In conclusion, we studied the wetting dynamics of superhydrophobic/superhydrophilic surfaces in the condition of bubbles scattered underwater. Unlike in air, a "coalescence delay" of the bubbles was observed under the studied conditions, and the delay time had a positive correlation with the
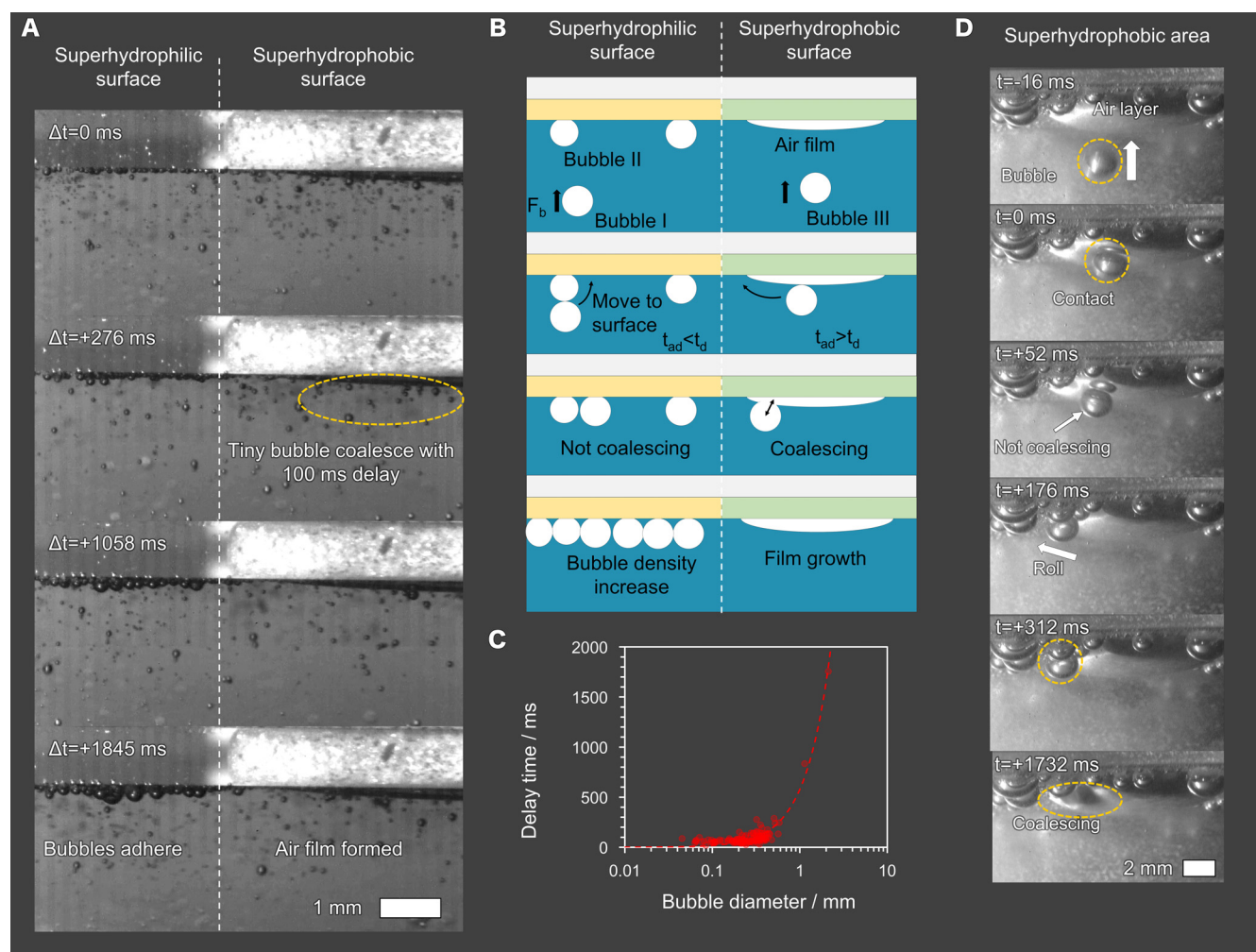
FIG. 3. Bubble adhesion dynamics on superhydrophobic and superhydrophilic surfaces. (a) Time-lapse images and (b) schematic illustrations of underwater scattered bubble deposition on the surfaces (left: superhydrophilic and right: superhydrophobic). (c) Bubble diameter versus coalescence delay time. The correlation coefficient was *ca.* 0.891. A plot is fitted by $t_d = 0.001r^3 + 14.0634r^2 + 563.954r^{1.5}$. (d) Time-lapse image of a large size bubble making impact with an air film formed on a superhydrophobic surface (controlled as $t_d < t_{ad}$).

bubble size. When penguins swim in the sea, flows of scattered bubbles are formed along the air layer.[9,22] This bubble scattering phenomenon can function as a drag reduction tool for penguins underwater. So far, the biomimetics for drag reduction relies on a simple air film formation,[23] yet the coalescence delay of bubbles strongly influences the interfacial energy change with time. Since this change can be converted to kinetic energy,[21] the influence of microbubbles on the drag reduction underwater cannot be negligible. We predict that the coalescence delay is a key to unravelling penguin-inspired wetting dynamics.

See supplementary material for the mechanism of gas generation by electrolysis, the structure of superhydrophobic coating, and the bubble adhesion behavior on superhydrophobic and superhydrophilic surfaces.

[1]X. Feng and L. Jiang, Adv. Mater. **18**, 3063 (2006).
[2]T. Darmanin and F. Guittard, J. Mater. Chem. A **2**, 16319 (2014).
[3]M. Tenjimbayashi and S. Shiratori, J. Appl. Phys. **116**, 114310 (2014).
[4]H. Dong, M. Cheng, Y. Zhang, H. Wei, and F. Shi, J. Mater. Chem. A **1**, 5886 (2013).
[5]G. McHale, M. I. Newton, and N. J. Shirtcliffe, Soft Matter **6**, 714 (2010).
[6]E. Jenner and B. D'Urso, Appl. Phys. Lett. **103**, 251606 (2013).
[7]S. Wang, Z. Yang, G. Gong, J. Wang, J. Wu, S. Yang, and L. Jiang, J. Phys. Chem. C **120**, 15923 (2016).
[8]W. Y. L. Ling, G. Lu, and T. W. Ng, Langmuir **27**, 3233 (2011).
[9]R. J. Daniello, N. E. Waterhouse, and J. P. Rothstein, Phys. Fluids **21**, 085103 (2009).
[10]C. Yu, P. Zhang, J. Wang, and L. Jiang, Adv. Mater. **29**, 1703053 (2017).
[11]R. Ma, J. Wang, Z. Yang, M. Liu, J. Zhang, and L. Jiang, Adv. Mater. **27**, 2384 (2015).
[12]X. Tian, V. Jokinen, J. Li, J. Sainio, and R. H. A. Ras, Adv. Mater. **28**, 10652 (2016).
[13]X. Chen, Y. Wu, B. Su, J. Wang, Y. Song, and L. Jiang, Adv. Mater. **24**, 5884 (2012).
[14]R. Xu, X. Xu, M. He, and B. Su, Nanoscale **10**, 231 (2018).
[15]C. Yu, M. Cao, Z. Dong, J. Wang, K. Li, and L. Jiang, Adv. Funct. Mater. **26**, 3236 (2016).
[16]M. E. Schrader, Langmuir **11**, 3585 (1995).
[17]M. Cao, J. Xiao, C. Yu, K. Li, and L. Jiang, Small **11**, 4379 (2015).
[18]J. De Ruiter, R. Lagraauw, D. Van Den Ende, and F. Mugele, Nat. Phys. **11**, 48 (2015).
[19]M. Tenjimbayashi, T. Matsubayashi, T. Moriya, and S. Shiratori, Langmuir **33**, 14445 (2017).

[20]X. Chen, R. S. Patel, J. A. Weibel, and S. V. Garimella, Sci. Rep. **6**, 18649 (2016).

[21]F. C. Wang, F. Yang, and Y. P. Zhao, Appl. Phys. Lett. **98**, 053112 (2011).

[22]P. J. Ponganis, R. P. Van Dam, G. Marshall, T. Knower, and D. H. Levenson, J. Exp. Biol. **203**, 3275 (2000).

[23]C. L. Williams, J. C. Hagelin, and G. L. Kooyman, Proc. R. Soc. B **282**, 20152033 (2015).